Asian Journal of Biochemistry

ISSN 1815-9923

Academic
Journals Inc.

www.academicjournals.com

Asian Journal of Biochemistry 1 (1): 84-97, 2006
ISSN 1815-9923

Morphology, Composition and Corrosion Properties of Electrodeposited Zn-Ni Alloys from Sulphate Electrolytes

M.M. Abou-Krisha, A.M. Zaky and A.A. Toghan
Department of Chemistry, Faculty of Science,
South Valley University, Qena, Egypt

Abstract: The electrodeposition of zinc-nickel alloys from sulphate bath has been studied using cyclic voltammetry technique, where some characteristics have been followed during both of the deposition and the dissolution of the alloys. Under the examined conditions, electrochemical and surface analysis indicate that the deposition has taken place with the formation of two structures have a composition corresponding to γ and δ phases of zinc-nickel alloy. Corrosion properties of Zn-Ni have been studied depending on the light of anodic linear polarization resistance technique. It is found that the protective capability of galvanic deposits containing Ni is substantially higher than that of ordinary Zn deposits. The effect of current density and sodium sulphate and boric acid concentrations on the morphology and the composition of the deposited films have been also studied. The results indicate that the deposition potential, morphology and the composition of the deposit have been greatly influenced by the current density. The Ni content in the deposition layer has been depressed at high current density, whereas, Zn deposition has been predominant. The increase of sodium sulphate in the bath significantly has increased the amount and content of Ni in the deposit and has decreased those of Zn. The addition of boric acid to the plating bath has increased the nucleation density of the deposit and consequently the content of Zn in the alloy. This effect has been attributed to the adsorptive interactions of boric acid at the electrode surface.

Key words: Electrodeposition, Zn-Ni alloy, anomalous codeposition, current density, boric acid, bath composition, sulphate bath, electrochemical studies

Introduction

Electroplated zinc coatings are considered as one main way for the corrosion protection of steel. Recently, the interest of Zn-Ni alloy coatings has increased owing to their better mechanical and corrosion properties compared with pure zinc coatings (Abou-Krisha, 2005; Bajat *et al*., 2000; Beltowska-Lehman *et al*., 2002; Brooks and Erb, 2001; Muller *et al*., 2002). Developing and studying electrolytes, from which Zn-Ni alloys are electrodeposited, is a high-priority problem in electroplating. The use of zinc and its alloys for improving the corrosion resistance of coated steel, has been growing worldwide (Bahrololoom *et al*., 2004; Sharples , 1990) and as a substitute for toxic and high-cost cadmium coatings (Alfantazi *et al*., 1996). In the automotive industry, for example, its use has been growing in search of increasing the corrosion resistance of chassis. The Zn-Ni alloys obtained by electrodeposition processes, with the amount of nickel varying between 8 and 14% by weight, give

Corresponding Author: M.M. Abou-Krisha, Department of Chemistry, Faculty of Science,South Valley University, Qena, Egypt Fax: 0020/96/5211279

corrosion protection five to six times superior to that obtained with pure zinc deposits (Anicai *et al*., 1992). Many studies have attempted to understand the characteristics of the deposition process of Zn-Ni alloy (Barcelo *et al*., 1994; Elkhatabi *et al*., 1996 a and b; Fabri Miranda *et al*., 1997; Koura *et al*., 2003; Muller *et al*., 2001, 1994; Roventi *et al*., 2000). The electrodeposition of Zn-Ni alloys is classified by Brenner (1963) as an anomalous codeposition where zinc, the less noble metal, is preferentially deposited. Although this phenomenon (Brenner, 1963) has been known since 1907, the codeposition mechanisms of zinc and nickel are not well understood (Mathias and Chapman, 1990; Swathirajan, 1987). There are some propositions to explain the anomalous codeposition of the Zn-Ni alloys. The first attributes the anomalous codeposition to a local pH increase, which would induce zinc hydroxide precipitation and would inhibit the nickel deposition (Fabri Miranda *et al*., 1997; Mathias and Chapman, 1990; Swathirajan, 1987). It has been, however, later that anomalous codeposition occurred even at low current densities (Keith Sasaki and Jan Talbot, 2000), where hydrogen formation is unable to cause large alkalinization effects. Another proposition is based on the underpotential deposition of zinc on nickel-rich zinc alloys or on nickel nuclei (Nicol and Philip, 1976; Swathirajan, 1986).

Two other propositions (Akiyama and Fukushima, 1992) on NiFe electrodeposition propose different mechanisms. The first mechanism assumes that Ni^{2+} discharges first to form a thin layer which chemisorbs water to form adsorbed $Ni(OH)^{+}$. Competition between the Ni^{2+} and Fe^{2+} to occupy active sites leads to the preferential deposition of Fe. Matlosz (1993) uses a two-step reaction mechanism involving adsorbed monovalent intermediate ions for both electrodeposition of iron and nickel, as single metals, and combines the two to develop a model for codeposition. Anomalous effects have been assumed to be caused by preferential surface coverage due to differences in Tafel rate constants for electrodeposition.

Sasaki and Talbot (2000) have proposed a model which extends the one-dimensional diffusion modeling of Grande and Talbot (1993), a supportive or interpretive, rather than a predictive, model of electrodeposition. A main contribution of this model is the inclusion of hydrogen adsorption and its effects on electrodeposition. Zech *et al*. (1999) have concluded that codeposition of iron group metals leads to a reduction of the reaction rate of the more noble component and an increase of the reaction rate of the less noble component compared to single metal deposition.

The aim of this research was to investigate the mechanism of Zn-Ni alloy deposition in sulfate electrolytes. Also the effect of different current density and sodium sulfate and boric acid concentrations of the plating bath, on the alloy composition and its dissolution resistance, and select an appropriate operating conditions to obtain an optimum nickel amount that provides best corrosion resistance of these types of alloy on steel substrate have been studied. The morphologies obtained of the different deposit types are presented, as well as an analysis of the deposit compositions. The results of the experimental approach have been based essentially on the analysis of the cathodic part of the cyclic voltammograms and galvanostatic measurements during electrodeposition and X-ray diffraction. The dissolution behavior of the deposits has been also investigated by using anodic linear polarization resistance and the anodic part of the cyclic voltammograms.

Materials and Methods

The electrolytes used for electrodeposition of Zn-Ni alloy have been freshly prepared by using Analar grade chemicals without further purification and doubly distilled water. The composition of the standard bath was 0.15 M H_3BO_3, 0.01 M H_2SO_4, 0.40 M Na_2SO_4, 0.20 M $NiSO_4$ and 0.20 M $ZnSO_4$ and the pH has been adjusted at 2.5.

Series of experiments have been carried out to study the effect of current density (1 to 30 mA cm^{-2}), sodium sulphate concentration (0.20 to 1.00 M) and boric acid concentration (0.15 to 0.60 M) of the bath on the deposits characteristics. To verify the influence of different conditions on the deposition process, a cyclic voltammetry behavior and galvanostatic measurement (Abou-Krisha, 2005) have been used. Anodic linear polarization for corrosion resistance studies has been also used (Abou-Krisha, 2005).

The electrochemical studies have been done with an EG and G potentiostat\galvanostat Model 237A, which is controlled by a PC using 352 corrosion software. The electrochemical cell has been composed of a steel rod (purity 99.98%) as a working electrode with a surface area of 0.196 cm^2, reference [Ag/AgCl/KCl(sat)] mounted in a Luggen capillary, and a Pt sheet which has been used as a counter electrode (Abou-Krisha, 2005). The cell has been filled with the 100 cm^3 of the electroplating solution of temperature 30.0°C and placed along the experiment in air thermostat to ensure adjustment of temperature at 30.0°C. All experiments have been duplicated and the reproducibility for this type of measurements has been found to be satisfactory. For standard bath we have made series of experiments at different times and the relative standard deviation (RSD %) has been obtained for Zn and Ni are 4.8 and 6.4% , respectively.

Scanning electron microscopy (SEM, JSM- 5500 LV, JEOL, Japan) has been used to study the morphology of the alloys and measure the thickness of the deposits (cross-section).

Atomic Absorption Spectroscopy (Variian SpectrAA 55) has been used to analyze coating composition. The Zn and Ni content in the deposit have been confirmed by EDS (Energy Dispersive X-ray Spectrometer) system with link Isis® software and model 6587 An X-ray detector (OXFORD, UK). From the resultant analysis, the film thickness and the cathode current efficiency of the deposit have been calculated.

The thickness of the deposited alloy layer has been approximately estimated from the amount of deposit and the densities of Zn (dZn = 7.14 g cm^{-3}) and Ni (dNi = 8.90 g cm^{-3}) of the same surface area (0.196 cm^2) (Abou-Krisha, 2005; Ohtsuka *et al*., 1995; Ohtsuka and Komori , 1998) and confirmed by SEM (cross-section).

X-ray diffractometry (XRD) model D5000 Siemens diffractometer has been used to identify the phases of Zn-Ni alloys deposited.

To measure the corrosion resistanceof the deposit, the linear polarization resistance technique has been used. In this technique the galvanostatically coated Zn-Ni on steel surface has been washed and transferred into the electrolytic cell containing 100.0 cm^3 0.025 M HCl in order to anodically dissolve the coating (Abou-Krisha, 2005). The values of electrochemical corrosion measurements of the coatings, $E_{(i = 0)}$- corrosion potential, I_{corr}- corrosion current, R_p- polarization resistance and corrosion rate, have been obtained and represented in Table 1-3.

Results and Discussion

Effect of current density

Figure 1 shows the potential-time dependence for the deposition of zinc-nickel alloys on steel substrate at different current densities. At low deposition current densities (1 mA cm^{-2}) the deposit consists of a high nickel-rich phase and the deposition has taken place with very low nucleation overpotential. This curve consists of two parts: the first part has indicated the deposition of Ni rich phase (Zn-Ni α-phase) which has needed the very low nucleation overpotential (i.e., normal codeposition).

Table 1: Compositions, thickness, current efficiencies and electrochemical corrosion measurements of the deposit on steel (0.196 cm^2) from a bath containing 0.20 M $ZnSO_4$, 0.20 M $NiSO_4$, 0.01 M H_2SO_4, 0.40 M Na_2SO_4 and 0.15 M H_3BO_3 at different current density for 10 min at 30.0°C.

Current density)	1	3	5	7	10	15	20	30
	---------- mA cm^{-2} ----------							
Ni amount in the deposit (10^{-6} g)	29.00	31.00	27.00	31.00	40.00	60.00	84.00	127.00
Zn amount in the deposit (10^{-6} g)	6.00	72.00	150.00	222.00	326.00	516.00	687.00	973.00
Total mass of the deposit (10^{-6} g)	35.00	103.00	177.00	253.00	366.00	576.00	771.00	1100.00
Ni content (%)	82.90	30.10	15.2.00	12.3.00	10.9.00	10.40	10.90	11.50
Zn content (%)	17.10	69.90	84.80	87.70	89.10	89.60	89.10	88.50
Zn-Ni deposit Current efficiency (e_{total}) (%)	96.20	89.10	90.40	92.00	93.00	97.50	97.90	3.20
Thickness of the deposit / µm	0.21	0.69	1.22	1.75	2.55	4.01	5.37	7.64
$i_{corr.}$ (A cm^{-2} x 10^{-3})	1.32	1.74	5.25	4.46	4.39	4.19	2.44	0.970
R_p (K-Ohms)	0.387	0.244	0.082	0.094	0.102	0.131	0.143	0.152
Corr. Rate (milli-inches $year^{-2}$)	336.00	706.00	2935.00	2450.00	2375.00	2237.00	1514.00	893.00
$E_{(I=0)}$ (mV)	-430.00	-743.00	-971.00	-969.00	-968.00	-965.00	-960.00	-948.00

Table 2: Compositions, thickness, current efficiencies and electrochemical corrosion measurements of the deposit on steel (0.196 cm^2) from a bath containing 0.20 M $ZnSO_4$, 0.20 M $NiSO_4$, 0.01 M H_2SO_4, different concentrations of Na_2SO_4 and 0.15 M H_3BO_3 at 10 mA cm^{-2} for 10 min at 30.0°C

Na_2SO_4 content in the bath (M)	0.20	0.40	0.60	0.80	1.00
Ni amount in the deposite (10^{-6} g)	25.00	41.00	60.00	77.00	95.00
Zn amount in the deposit (10^{-6} g)	304.00	294.00	284.00	2750.00	265.00
Total mass of the deposit (10^{-6} g)	329.00	335.00	344.00	352.00	360.00
Ni content (%)	7.60	12.2.00	17.40	21.90	26.40
Zn content (%)	92.40	87.80	82.60	78.10	73.60
Zn-Ni deposit Current efficiency (e_{total}) (%)	83.30	85.30	88.10	90.50	93.10
Thickness of the deposit / µm	2.31	2.32	2.36	2.39	2.42
$i_{corr.}$(A cm^{-2}x10^{-3})	4.32	4.18	3.87	3.54	3.10
R_p (K-Ohms)	0.110	0.114	0.119	0.121	0.128
Corr. Rate (milli-inches $year^{-1}$)	2318.00	2255.00	2199.00	2121.00	1917.00
$E_{(I=0)}$ (mV)	-968.00	-961.00	-955.00	-952.00	-0943.00

Table 3: Compositions, thickness, current efficiencies and electrochemical corrosion measurements of the deposit on steel (0.196 cm^2) from a bath containing 0.20 M $ZnSO_4$, 0.20 M $NiSO_4$, 0.01 M H_2SO_4, 0.40 M Na_2SO_4 and different concentrations of H_3BO_3 at 10 mA cm^{-2} for 10 min at 30.0°C

H_3BO_3 concentration in bath (M)	Without	0.15	0.30	0.45	0.60
Ni amount in the deposit (10^{-6}g)	36.00	36.00	37.00	37.00	37.00
Zn amount in the deposit (10^{-6}g)	279.00	314.00	333.00	343.00	357.00
Total mass of the deposit (10^{-6}g)	315.00	350.00	370.00	380.00	394.00
Ni content (%)	11.40	10.30	10.00	9.70	9.40
Zn content (%)	88.60	89.70	90.00	90.30	90.60
Zn-Ni deposit Current efficiency (e_{total}) (%)	80.10	88.90	94.00	96.50	99.90
Thickness of the deposit / µm	2.19	2.44	2.58	2.65	2.75
$i_{corr.}$ (A cm^{-2} x 10^{-3})	4.59	4.21	3.22	2.35	1.98
R_p (K-Ohms)	0.094	0.118	0.128	0.141	0.159
Corr. Rate (milli-inches $year^{-2}$)	2510.00	2221.00	1925.00	1834.00	1716.00
$E_{(I=0)}$ (mV)	-970.00	-966.00	-961.00	-958.00	-949.00

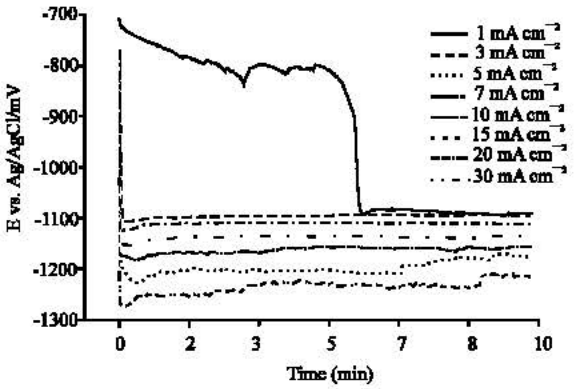

Fig. 1: E-t curves for steel in 0.20 M $ZnSO_4$, 0.20 M $NiSO_4$, 0.01M H_2SO_4, 0.40 M Na_2SO_4 and 0.15 M H_3BO_3 at different current density for 10 min at 30.0°C

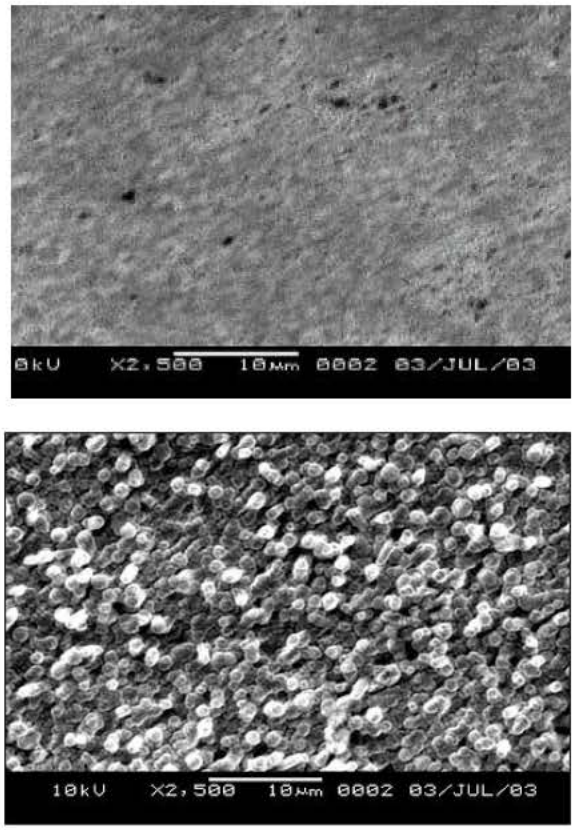

Fig 2: SEM photographs of electrodeposited Zn-Ni on steel from a bath containing 0.20 M $ZnSO_4$, 0.20 M $NiSO_4$, 0.01 M H_2SO_4, 0.40 M Na_2SO_4 and 0.15 M H_3BO_3 at different current density for 10 minutes at 30.0°C. (a) at 1 mA cm^{-2}. (b) at 10 mA cm^{-2}

The second part corresponds to an increase in Zn content (which induced by the deposited Ni (Fabri Miranda *et al*., 1997)), due to a formation of new Zn-Ni phases (probably γ-phase), which have been indicated by the sharp increase in the nucleation overpotential. The morphology of the deposits is very similar to α-phase deposits as shown in Fig. 2a. The alloy formed with current density (1 mA cm^{-2}) shows a very uniform structure, which has appeared less, deformed even at higher magnification, and very similar to that of pure Ni electrodeposits (Kalantary *et al*., 1998). As the current density has increased (3-7 mA cm^{-2}), more overpotential is needed to create the initial nucleus and more zinc is deposited, but the deposit can still grow at low potentials. At these low polarizations, the deposition of nickel has been strongly inhibited by the presence of zinc while the deposition of zinc has been induced by the presence of nickel (Fabri Miranda *et al*., 1997; Zech *et al*., 1999). As current density has increased (10-20 mA cm^{-2}) more overpotential is necessary to create the first nucleus and more zinc is deposited. This means that at the higher current densities the deposition has taken place at overpotentials related to the deposition potential of Zn. When the zinc content has increased (Table 1) at current density 10 mA cm^{-2}, a grain deposit with a smaller and similar size crystal (Fig. 2b) has been obtained. All these conditions correspond to zinc deposited at potentials below its deposition potential where the reduction of this metal has been driven by the Ni^{2+} deposition. The increase of current density up to 30 mA cm^{-2} leads to rise of the potential to plateau slightly and then slowly relaxes to more positive values after the nucleation spike. When the deposits obtained in this zone have been analyzed, Zn contents of about 89% have been obtained.

The effects of current density on the percentage of Ni and Zn in Zn-Ni alloys from sulphate bath are shown in Table 1. At low current density there is a relatively high Ni content in the alloy, which results from the more noble nature of Ni (normal-codeposition). However, the decrease in Ni content when current density increased has been observed. A small rise in Ni content can be observed at the higher current density employed because the preferentially deposited Zn (less noble metal) is more depleted in the cathode diffusion layer than the Ni (more noble metal). Also, current efficiency of the alloy which has been increased generally is due to the increase of the Zn content, which represents the main alloy component. Increase in the thickness of the deposited layer follows these changes. This may be due to the increase of Zn content on the alloy which possesses the lower density. Also, it is obvious that at current density values higher than 5 mA cm^{-2} the composition of the formed Zn-Ni alloy has taken almostly constant value.

Linear polarization resistance tests (Fig. 3 as a representative results) have been done using galvanostatically coated steel by Zn-Ni alloys. It is observed that (Table 1) at low

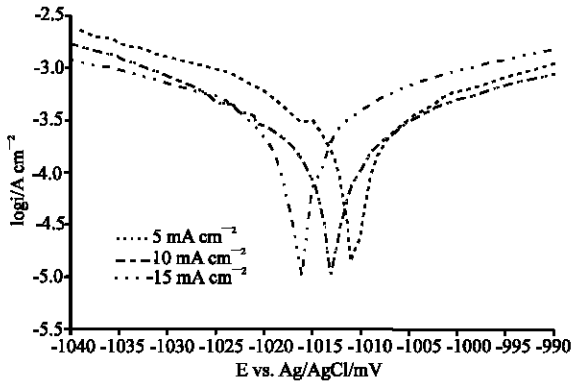

Fig. 3: log i-E curves for steel, plated from a bath containing 0.20 M $ZnSO_4$, 0.20 M $NiSO_4$, 0.01M H_2SO_4, 0.40 M Na_2SO_4 and 0.15 M H_3BO_3 at different current density for 10 min at 30.0°C, in 0.025 M HCl at 30.0°C

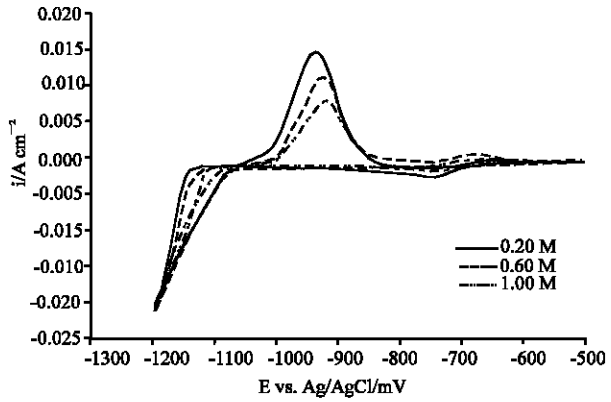

Fig.4: i-E curves (cyclic voltammograms) for steel in 0.20 M $ZnSO_4$, 0.20 M $NiSO_4$, 0.01M H_2SO_4, different concentrations of Na_2SO_4 and 0.15 M H_3BO_3 and scan rate 5 mV s^{-1} at 30.0°C

current density (1 mA cm^{-2}) a normal codeposition has taken place and has been detected by the higher Ni content in the deposit. Therefore, the measured corrosion potential has more positive value and the alloy has a better corrosion-resistance. As the current density has increased to 3 mA cm^{-2}, the $E_{(i=0)}$ has shifted negatively due to the decrease of Ni content. Also, the increase of the current density from 5 to 30 mA cm^{-2}, the measured corrosion potential has shifted positively. This is, may be, owing to the increase of the amount of Zn and Ni in the alloy and the thickness of the deposited by increasing the deposition current density. From the values of electrochemical corrosion measurements we can conclude that the corrosion rate and current have decreased and the polarization resistance has increased with the current density increased from 5-30 mA cm^{-2}. While, at low currents (1-3 mA cm^{-2}), these values depending on the Ni content in the deposit, have taken the opposite direction with the current density increased.

Effect of Na_2SO_4 Concentration

The influence of the Na_2SO_4 concentrations on the cyclic voltammograms has been studied. It indicate that the deposition potentials have shifted positively when the Na_2SO_4 concentration in the electrolyte has increased due to the increase of deposited Ni content in the alloy (Fig. 4 and Table 2). At the same time the cathodic peak, which starts at about -0.5 V, has decreased when Na_2SO_4 concentration has increased attributed to the hydrogen evolution decreases and this appears as increasing the current efficiency of the deposit (Abou-Krisha, 2005).

From the anodic part of the cyclic voltammograms it seems that, the phases of the Zn-Ni alloys varied with Na_2SO_4 concentration. These phases are δ-phase [(Ni_3Zn_{22}) the first dissolution anodic peak] and γ [(Ni_5Zn_{21}) the second dissolution anodic peak], which are ascribed to the preferential dissolution of Zn from two phases. In the presence of 0.20 M Na_2SO_4, the γ-phase has been the lowest quantity and the δ-phase has been the highest quantity comparable with the other Na_2SO_4 additions. This result is confirmed by XRD (Fig. 5a and b) which indicates that increasing Na_2SO_4 concentration in

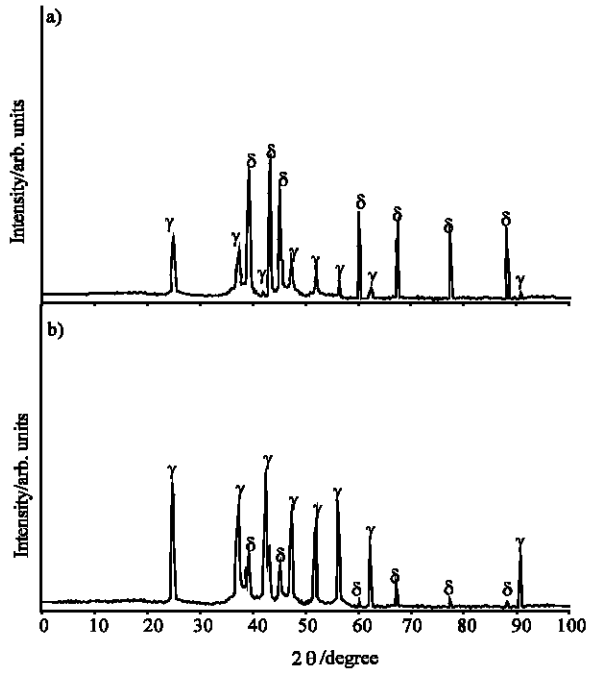

Fig. 5: XRD patterns of electrodeposited Zn-Ni on steel, obtained at potential -1.13 V. holds for 15 min from a bath containing 0.20 M $ZnSO_4$, 0.20 M $NiSO_4$, 0.01 M H_2SO_4, different concentrations of Na_2SO_4 and 0.15 M H_3BO_3 at 30.0°C. (a) at 0.20 M Na_2SO_4. (b) at 0.60 M Na_2SO_4

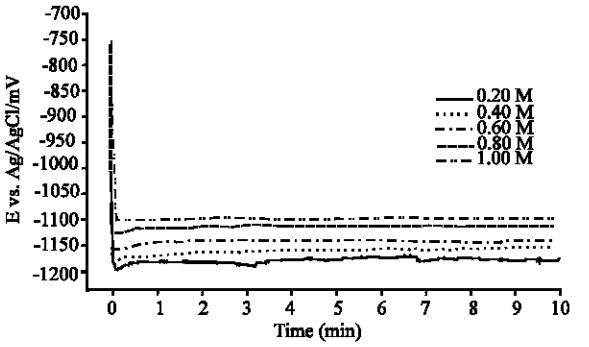

Fig. 6: E-t curves for steel in 0.20 M $ZnSO_4$, 0.20 M $NiSO_4$, 0.01M H_2SO_4, different concentrations of Na_2SO_4 and 0.15 M H_3BO_3 at 10 mA cm^{-2} for 10 min at 30.0°C

the bath, the γ-phase has increased and the δ-phase has decreased in the deposit. The main reason for this behavior could be attributed to the increase of electrolyte conductance as a result of adding Na_2SO_4 and hence would induce the deposition of Ni.

Galvanostatic measurements also indicate that the cathodic deposition potentials have shifted positively by increasing Na_2SO_4 concentrations (Fig. 6). Also, it is noticed that more overpotential has been needed to create the first nucleus with decreasing Na_2SO_4 concentrations. From Table 2 it is clear that the rising Na_2SO_4 concentrations significantly have increased Ni amount and its content in the deposit. On the other hand, Zn amount and its content in the deposit has decreased. When Na_2SO_4 concentrations maintained between 0.20 to 1.00 M at current density 10 mA cm^{-2}, deposits with 7.5-26.5% nickel content have been readily obtained and the current efficiency of alloy deposition can reach 93%. Also, there is a little increase in the thickness comparable, as expected, with the increasing of the total mass. This is ascribed to the total mass increases as the increases of Ni content which possesses the higher density than Zn.

It is quite clear that uniform deposit Fig. 2b has been obtained from bath containing 0.40 M Na_2SO_4 concentration. Curiously, the most uniform deposit with a similar small grain size has been observed, as Na_2SO_4 concentration has been raised to 0.60 M (Fig. 7) owing to the increase of Ni and Zn content.

Linear polarization tests have been done using galvanostatically coated steel by Zn-Ni alloy. From Table 2 it seems that increasing Na_2SO_4 concentration, the corrosion rate, potential and current have decreased and polarization resistance has increased. This indicates that corrosion-resistance has increased by increasing the Na_2SO_4 concentration.

Effect of H_3BO_3 concentration

The role of boric acid has been of great interest in the electrodeposition of Ni (Hoare, 1986) and Zn alloys (Karwas and Hepel, 1989). It is now believed that boric acid either complexes with Ni^{2+}, acting as a homogeneous catalyst, or adsorbs on the electrode surface, has a significant role in morphology and compositional characteristics. The presence of boric acid results in an increase of current efficiency of deposition process, amount of Zn in the deposited alloy, and the nucleation density of the deposit (Karwas and Hepel, 1989). These effects have been attributed to the adsorptive

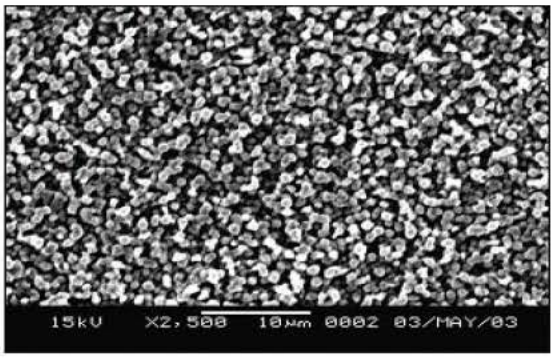

Fig. 7: SEM photographs of electrodeposited Zn-Ni on steel from a bath containing 0.20 M $ZnSO_4$, 0.20 M $NiSO_4$, 0.01M H_2SO_4, 0.60 M Na_2SO_4 and 0.15 M H_3BO_3 at 10 mA cm^{-2} for 10 min at 30.0°C

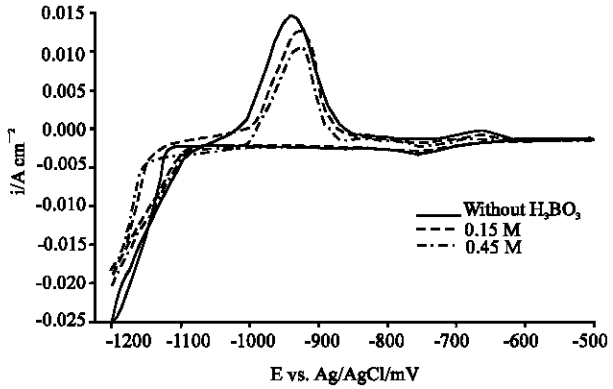

Fig. 8: i-E curves (cyclic voltammograms) for steel in 0.20M $ZnSO_4$, 0.20 M $NiSO_4$, 0.01M H_2SO_4, 0.40 M Na_2SO_4 and different concentrations of H_3BO_3 and scan rate 5 mV s^{-1} at 30.0°C

interactions of boric acid at the electrode surface. Also, boric acid acting as buffer to maintain the pH of the electrolyte bath (Abou-Krisha, 2005; Lin and Selman, 1993; Velichenko *et al*., 1999). Similar effects of boric acid have been observed in the present work during Zn-Ni deposition from suggested sulphate bath.

The influence of the boric acid concentration on the cathodic part of the cyclic voltammograms has been studied, as shown in Fig. 8. In these curves the deposition potentials have been shifted negatively, where the boric acid concentration in the electrolyte has increased due to the increase of Zn deposited and the decrease of deposited Ni content in the alloy (Table 3). Also, the cathodic peak, which starts at about -0.5 V, attributable to probably the presence of H_2SO_4 and consequently the hydrogen evolution, has decreased with boric acid concentration increases. This may be due to that the boric acid acts as a buffer solution. Also, this may be ascribed to the adsorption of the boric acid on the electrode surface and in turn has decreased the surface coverage by H^+ with increasing its concentration.

It is found, from the anodic part of the cyclic voltammograms, that the phases of the deposits obtained, from solutions containing different boric acid concentrations, have consisted of a mixture of two phases (δ and γ). In spite of the little Zn content deposited in the absence of boric acid, the two anodic peaks have approximately appeared at-0.97 V and -0.64 V have the highest peaks, due to the highest cathodic charge. Whereas, in the presence of boric acid the two anodic peaks generally have shifted to more positive potentials (i.e., the dissolution resistance has increased). This observation has been attributed to the adsorptive interactions of boric acid at the electrode surface, which have increased Zn amount in the deposit. The peak height has decreased with increasing boric acid concentrations, although Zn content has increased in the deposit as increasing boric acid concentrations. This is due to a parallel decrease of cathodic charge. Due to the increase of nucleation overpotential, at constant E_{inv} the deposition cathodic charge has diminished.

Figure 9 shows the potiental-time dependencefor the deposition of Zn-Ni alloys on steel at different boric acid concentration.This Fig. 9 has indicated that the cathodic deposition potentials have shifted negatively by increasing boric acid concentrations. It seems that as increasing the concentrations of boric acid, more overpotential has been needed to create the initial nucleus and more zinc has been deposited, after the nucleation spike.

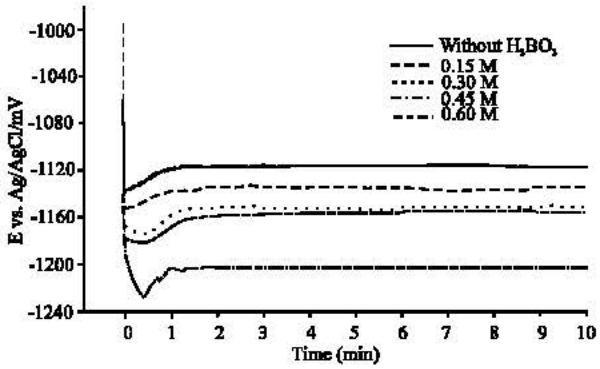

Fig. 9: E-t curves for steel in 0.20 M $ZnSO_4$, 0.20 M $NiSO_4$, 0.01 M H_2SO_4, 0.40 M Na_2SO_4 and different concentrations of H_3BO_3 at 10 mA cm^{-2} for 10 min at 30.0°C

From Table 3 it is significantly clear that, as increasing the boric acid concentration in the bath, an increase of the Zn content and smaller decrease of the Ni content in the deposited alloy layer has taken place. The alloy current efficiency has increased due to the decrease of the hydrogen ions adsorption and increase of the total mass of the deposit. Also, the thickness of the deposited film has increased owing to that the amount of Zn, which is the main content and possesses the lower density, has increased.

The morphology of zinc-nickel alloys on steel electrode has been influenced by the boric acid concentrations. The results indicate that adding boric acid to plating bath has increased the nucleation density of the deposit and increased the amount of Zn deposited. Fig. 10 has confirmed that the increase of boric acid has produced a more refined grain structure comparable with Fig. 2b. This reduction in grain size can be explained by the increase of deposited film, which increases the number of new grains nucleated.

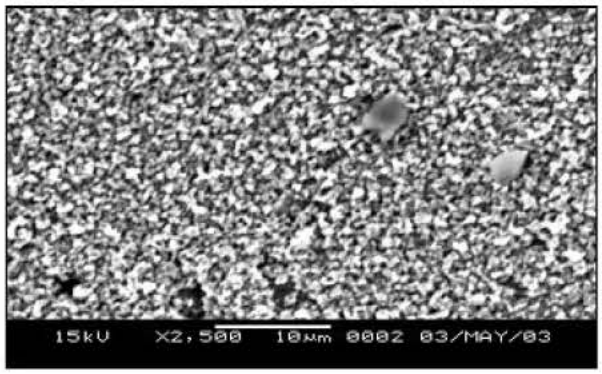

Fig. 10: SEM photographs of electrodeposited Zn-Ni on steel from a bath containing 0.20 M $ZnSO_4$, 0.20 M $NiSO_4$, 0.01M H_2SO_4, 0.40 M Na_2SO_4 and 0.30 H_3BO_3 at 10 mA cm^{-2} for 10 minutes at 30.0°C

It is observed from Linear polarization tests that, the Zn-Ni alloy coatings obtained by different boric acid concentrations have shown that the corrosion potential has decreased, when the boric acid concentration has increased (Table 3), comparable to the corrosion potential value (E(i = 0). = -1.062 V) of electrodeposited pure Zn on steel (Kalantary *et al*., 1998). The electrochemical corrosion measurements has indicated that the corrosion rate and current have decreased and the polarization resistance has increased with the boric acid concentration increased. Thus, the improvement achieved in the corrosion resistance of deposits can be explained by its different morphology, as well as its refined grains, the composition of the alloy and the thickness can be considered as the reasons for the results obtained with electrodeposits in this work.

Thus, based on the results in Table 1-3, it is possible to select an appropriate operating conditions to obtain an optimum nickel concentration in the range of 11-13% that provides best corrosion resistance for these types of alloy on steel substrate (Short *et al*., 1989).

Conclusions

In the present research a sulphate bath has been used and Zn-Ni alloy deposits have been obtained at different variables such as current density, and concentration of sodium sulphate and boric acid in the bath. The morphologies obtained of the different deposit types are presented, as well as an analysis of the deposit compositions. Different proportions of the two metals can be obtained by using different deposition parameters, but at all, preferential deposition of zinc occurs and anomalous codeposition has taken place. The results suggest the following sequence of events: first, Ni^{2+} (or its monovalent intermediate) adsorbed; followed by adsorption of Zn^{2+} (or its monovalent intermediate) onto the freshly adsorbed and deposited nickel. The adsorption of zinc ions inhibit subsequent deposition of nickel, although it does not block it completely. Electrochemical tests results are also presented in order to verify the corrosion behavior of deposits.

At low deposition current densities (1 mA cm^{-2}) the deposit consists of a high nickel-rich phase and the deposition has taken place with very low nucleation overpotential. The deposition process consists of two parts, the first part indicates the deposition of Ni rich phase (ZnNi α-phase) which needed the very low nucleation overpotential (i.e. normal codeposition). The second part corresponds to an increase in Zn content (which induced by the deposited Ni), due to the formation of new ZnNi phases (probably γ-phase), and indicated by the sharp increase in the nucleation overpotential.

The deposition potentials have shifted positively when the Na_2SO_4 concentration in the electrolyte has increased due to the increase of deposited Ni content in the alloy. In the presence of 0.20 M Na_2SO_4, the γ-phase has been the lowest quantity and the δ-phase has been the highest one comparable to other Na_2SO_4 concentrations. The addition of boric acid has raised the Zn amount in the deposited alloy, has increased the nucleation density of the deposit and has produced more refined grain structure.

It is interesting to mention that the current efficiency has generally increased, as can be seen in Table 2 and 3, due to the decrease of H^+ adsorbed and in turn the hydrogen evolution decreases, as the boric acid and sodium sulphate concentrations have increased. On the other hand, from Table 1, the current efficiency has decreased when the current density has changed from 1 to 3 mA cm^{-2}. This is because at low current density the adsorbed H^+ and consequently the hydrogen evolution is very low and has increased by increasing the current density. Increasing the current density from 3-15 mA cm^{-2}, there is a competition between the increase of H^+ adsorption and the activation of Ni^{2+} and Zn^{2+} adsorption, which is predominant, and reaches limitation at 15 mA cm^{-2}. At higher current densities than 15 mA cm^{-2} the H^+ adsorption has increased.

References

Akiyama, T. and H. Fukushima, 1992. Recent study on the mechanism of the electrodeposition of iron-group metal alloys. ISIJ Intl., 32: 787-798.

Anicai, L., M. Siteavu and E. Grunwald, 1992. Corrosion behaviour of zinc and zinc alloy depositions. Corros. Prevent. Control, 39: 89-93

Alfantazi, A.M., J. Page and U. Urb, 1996. Pulse plating of Zn-Ni alloy coatings. J. Applied Electrochem., 26: 1225-1234.

Abou-Krisha, M.M., 2005, Electrochemical studies of zinc–nickel codeposition in sulphate bath. J. Applied Surf. Sci., 252: 1035-1048.

Brenner, A., 1963, Electrodeposition of Alloys. Vol. 2, Academic Press, New York, pp: 194.

Barcelo, G., J. Garcia, M. Sarret, C. Muller and J. Pregonas, 1994. Properties of Zn-Ni alloy deposits from ammonium baths. J. Applied Electrochem., 24: 1249-1255.

Bajat, J. B., Z. Kacarevic-Popovic, V.B. Miskovic-Stankovic and M.D. Maksimovic, 2000. Corrosion behaviour of epoxy coatings electrodeposited on galvanized steel and steel modified by Zn-Ni alloys. Progr. Org. Coat., 39: 127-135.

Brooks, I. and U. Erb, 2001. Hardness of electrodeposited microcrystalline and nanocrystalline γ-phase Zn-Ni alloys. Scripta Mater., 44: 853-858.

Beltowska-Lehman, E., P. Ozga, Z. Swiatek and C. Lupi, 2002. Electrodeposition of Zn–Ni protective coatings from sulfate–acetate baths. Surf. Coat. Technol., 151: 444-448.

Bahrololoom, M.E., D.R. Gabe and G.D. Wilcox, 2004. Microstructure, morphology and corrosion resistance of electrodeposited zinc-cobalt compositionally modulated alloy multilayer coatings. Trans. IMF, 82: 51-58.

Elkhatabi, F., G. Barcelo, M. Sarret and C. Muller, 1996a. Electrochemical oxidation of zinc + nickel alloys in ammonium baths. J. Electroanal. Chem., 419: 71-76.

Elkhatabi, F., M. Sarret and C. Muller, 1996b. Chemical and phase compositions of zinc + nickel alloys determined by stripping techniques. J. Electroanal. Chem., 404: 45-53.

Fabri Miranda, F.J., O.E. Barcia, O.R. Mattos and R.Wiart, 1997. Electrodeposition of Zn-Ni alloys in sulfate electrolytes. I. Experimental approach. J. Electrochem. Soc., 144: 3441-3449.

Grande, W.C. and J.B. Talbot, 1993. Electrodeposition of thin films of nickel-iron. II. Modeling. J. Electrochem. Soc., 140: 675-681.

Hoare, J.P., 1986, On the role of boric acid in the watts bath, J. Electrochem. Soc., 133: 2491-2495.

Karwas, C. and T. Hepel, 1989. Morphology and composition of electrodeposited cobalt-zinc alloys and the influence of boric acid. J. Electrochem. Soc., 136: 1678-1672

Kalantary, M.R., G.D. Wilcox and D. R. Gabe, 1998. Alternative layers of zinc and nickel electrodeposited to protect steel. Br. Corrosion J., 33: 197-201.

Keith Sasaki, Y. and B. Jan Talbot, 2000. Electrodeposition of iron-group metals and binary alloys from sulfate baths. II. modeling. J. Electrochem. Soc., 147: 189-197.

Koura, N., Y. Suzuk, Y. Idemoto, T. Kato and F. Matsumoto, 2003. Electrodeposition of Zn-Ni alloy from $ZnCl_2$-$NiCl_2$-EMIC and $ZnCl_2$-$NiCl_2$-EMIC-EtOH ambient-temperature molten salts, Surf. Coat. Technol., 169: 120-123.

Lin, Y. and J.R. Selman, 1993. Electrodeposition of Ni-Zn alloy. II. Electrocrystallization of Zn, Ni and Ni-Zn alloy. J. Electrochem. Soc., 140: 1304-1311.

Mathias, M.F. and T.W. Chapman, 1990. Estimating kinetics parameters for nickel-zinc alloy deposition from current distribution measurements on the rotating disk electrode. J. Electrochem. Soc., 137: 102-110.

Matlosz, M., 1993. Competitive adsorption effects in the electrodeposition in iron-nickel alloys. J. Electrochem. Soc., 140: 2272-2279.

Muller, C., M. Sarret and M. Benballa, 2001. Some peculiarities in the codeposition of zinc-nickel alloys, Electrochim. Acta, 46: 2811-2817.

Muller C., M. Sarret and M. Benballa, 2002. Complexing agents for a Zn-Ni alkaline bath. J. Electroanal. Chem., 519: 85-92.

Nicol, M.J. and H.I. Philip, 1976. Underpotential deposition and its relation to the anomalous deposition of metals in alloys. J. Electroanal. Chem., 70: 233-237.

Ohtsuka, T., E. Kuwamura, A. Komori and T. Uchida, 1995. Ellipsometric study of the initial layer formation of the preferential Zn deposition in Zn-Ni electroplating. ISIJ Intl., 35: 892-899.

Ohtsuka, T. and A. Komori, 1998. Study of initial layer formation of Zn–Ni alloy electrodeposition by in situ ellipsometry, Electrochim. Acta, 43: 3269-3276.

Roventi, G., R. Fratesi, R.A.Della Guardia and G. Barucca, 2000. Normal and anomalous codeposition of Zn-Ni alloys from chloride bath. J. Applied Electrochem., 30: 173-179.

Swathirajan, S., 1986. Potentiodynamic and galvanostatic stripping methods for characterization of alloy electrodeposition process and product. J. Electrochem. Soc., 133: 671-680.

Swathirajan, S., 1987. Electrodeposition of zinc + nickel alloy phases and electrochemical stripping studies of the anomalous codeposition of zinc. J. Electroanal. Chem., 221: 211-228.

Short, N., A. Abibsi and J. K. Dennis, 1989. Corrosion resistance of electroplated zinc alloy coatings. Trans. IMF, 67: 73-77.

Sharples, T. E., 1990. Zn-Co: Fighting corrosion in the 90's. Prod. Finish., 54: 38-44.

Velichenko, A.B., J. Portillo, M. Sarret and C. Muller, 1999, Surface analysis of films formed on a zinc anode in Zn-Ni electroplating bath. J. Appl. Surf. Sci., 148: 17-23.

Zech N., E.J. Poldlaha and D. Landolt, 1999. Anomalous codeposition of iron group metals. I. Experimental results. J. Electrochem. Soc., 146: 2886-2891.